Identification of a Glycosaminoglycan Binding Surface on Human Interleukin-8

Gabriele S. V. Kuschert,[‡] Arlene J. Hoogewerf,[§,||] Amanda E. I. Proudfoot,[§] Chun-wa Chung,[⊥] Robert M. Cooke,[⊥] Roderick E. Hubbard,[‡] Timothy N. C. Wells,*[,§] and Paul N. Sanderson*[,⊥]

Department of Chemistry, University of York, Heslington, York YO1 5DD, United Kingdom, Geneva Biomedical Research Institute, Glaxo Wellcome Research and Development SA, 14, chemin des Aulx, 1228 Plan-les-Ouates, Geneva, Switzerland, and Glaxo Wellcome Medicines Research Centre, Gunnels Wood Road, Stevenage, Hertfordshire, SG1 2NY, United Kingdom

Received November 24, 1997; Revised Manuscript Received March 23, 1998

ABSTRACT: The activation of leukocytes by chemokines is believed to be mediated *via* binding of chemokines to glycosaminoglycan chains of the extracellular matrix. The binding site on the chemokine interleukin-8 (IL-8) for the glycosaminoglycan heparin has been characterized using a systematic series of site-directed mutants of IL-8 in which the basic residues of the protein have been replaced by alanine. Mutation of K64 and R68 caused the largest decrease in affinity for a heparin Sepharose matrix, with smaller effects seen with mutations of K20, R60, and K67. Heparin-derived disaccharides that could disrupt the IL-8-heparin Sepharose interaction were identified by a competitive binding assay. Heteronuclear NMR spectroscopic titration of ^{15}N-labeled IL-8 with a trisulfated disaccharide revealed a cluster of residues on IL-8 which were perturbed by disaccharide binding. These data identify a heparin-binding surface on IL-8 that includes the C-terminal α-helix and the proximal loop around residues 18−23. The heparin-binding site is spatially distinct from the residues involved in receptor binding.

Interleukin-8 (IL-8)[1] is one of a superfamily of inflammatory proteins, called chemokines, which are involved in the chemotaxis and activation of leukocytes in damaged or infected tissues (*1*). IL-8 is an 8 kDa protein and is the best characterized of the α (or CXC) class of chemokines which mediate acute inflammatory reactions mainly via neutrophil attraction and activation (*2*). The activation of leukocytes by chemokines requires binding to specific G-protein-coupled "seven transmembrane helix" receptors (*3*). Chemokines can also bind to the glycosaminoglycan (GAG) chains of proteoglycans present at the vascular endothelial surface and in the extracellular matrix. The biological role of the chemokine−GAG complex is not clear: it may assist the presentation of chemokines to receptors, help create an immobilized chemokine concentration gradient required for chemoattraction, or sequester the chemokine in an inactive form (*4*). Although the CXC chemokines are active as monomers (*5*) they can dimerize at higher concentrations (*6*). Recently, GAGs have been shown to mediate cell surface oligomerization of chemokines in vitro (*7*) and may exert similar effects *in vivo*.

Glycosaminoglycans are polyanionic polysaccharide constituents of cell surface and extracellular matrix proteoglycans that are involved in a multitude of intermolecular interactions (*8*). One important family of GAGs, the heparan sulfates, is structurally heterogeneous as a result of postpolymerization modifications, including sulfation and epimerization, of the precursor (glucuronate−glucosamine) copolymer (*9*). Interactions of proteins with both heparan sulfates (and the closely related but generally more highly sulfated heparins (*10*)) may be highly specific for particular saccharide sequences (*9*). It has been shown for both fibronectin (*11*) and basic fibroblast growth factor (bFGF) (*12*) that the specificity is conferred by highly sulfated domains, which are interspersed with less sulfated regions within heparan sulfates (*13*, *14*). The binding of heparin to bFGF facilitates both oligomerization and receptor binding (*15*), and bFGF complexed with a heparin-derived decasaccharide is biologically active (*16*). Structural insight into this interaction has been extrapolated from crystallographic studies of bFGF complexed with heparin-derived tetra- and hexa-saccharides (*17*), and with nonsulfated di- and tri-saccharides which are capable of binding to bFGF and activating the bFGF signaling pathway (*18*).

The differential binding of chemokines to GAG subpopulations has been demonstrated by affinity co-electrophoresis (*19*) and by direct binding (*7*). Models of GAG-CXC chemokine complexes (*20*) have been proposed on the basis of NMR and X-ray structures of the proteins (*21*, *22*); however, no direct experimental details of the structure of chemokine-GAG complexes exist. The basic residues of platelet factor 4 (PF4) which are involved in binding to heparin have been identified by site-directed mutagenesis and NMR (*23*), and specific saccharide sequences in heparan sulfates that are required for PF4 binding have also recently been characterized (*24*). In common with PF4 the C-terminal helix of IL-8 has been implicated in heparin binding by

* Corresponding Authors.
[‡] University of York.
[§] Glaxo Wellcome Research and Development SA.
[||] Present address: Midland Certified Reagent Company, 3112A West Cuthbert Avenue, Midland, TX 79701.
[⊥] Glaxo Wellcome Medicines Research Centre.

[1] Abbreviations: IL-8, interleukin-8; GAG, glycosaminoglycan; bFGF, basic fibroblast growth factor; PF4, platelet factor 4; HEPES, (*N*-[2-hydroxyethyl]piperazine-*N*′-[2-ethanesulfonic acid]); HSQC, heteronuclear single quantum correlation; SPA, scintillation proximity assay.

S0006-2960(97)02867-5 CCC: $15.00
Published on Web 07/24/1998

truncation of synthetic versions of the protein (*25*). This region is distinct from that required for receptor binding which includes the amino-terminal ELR motif (*26*, *27*) and a hydrophobic epitope (*28*, *29*). In this report we describe a combined site-directed mutagenesis, affinity chromatography and NMR study in which we have identified the residues of IL-8 involved in GAG binding.

EXPERIMENTAL PROCEDURES

Materials. Heparin disaccharides listed in Table 3 (as sodium salts, except **IV**−**H** which was the free acid) were obtained from Sigma, as was the S-Sepharose (fast-flow). Sepharose CL-6B, heparin Sepharose CL-6B, Sephacryl S200 HR, HiLoad SP Sepharose, and HiLoad Phenyl Sepharose were from Pharmacia. HEPES buffer was from Life Technology. Recombinant IL-8 was expressed in *Escherichia coli* and purified as described previously (*30*). [^{125}I]IL-8 was obtained from Amersham (specific activity 2000 Ci/mmol). ^{15}N-labeled human IL-8 was from VLI Research (Audubon PA) and was estimated to be at least 83% ^{15}N by electrospray mass spectrometry. Deuterium oxide (99.98% D) was from Aldrich. All other reagents were of laboratory grade.

Mutagenesis. A gene encoding mature human IL-8 was inserted into the *E. coli* expression vector pET23d. Mutants were constructed using Transformer site-directed mutagenesis (Clonetech, Palo Alto, CA) according to the manufacturer's protocol. Briefly, pET23d-encoding IL-8 was denatured and annealed with a *Xba*I unique selection primer and the desired mutation primer. Primers were elongated and ligated using T4 DNA ligase for 2 h. The mutagenic plasmid was digested with *Xba*I for 2 h at 37 °C and transformed into BMH 71−18 mut S *E. coli* strains. The amplified DNA was purified and digested with *Xba*I for second round selection. The digested mixture was then transformed into the *E. coli* strain JM109. The desired mutation was verified by DNA sequencing prior to expression.

Mutant Expression and Protein Purification. Mutant proteins were produced in which each of the basic residues was mutated to alanine. Expression vectors containing the T7 promoter were transformed into the BL21 (DE3) *E. coli* strain. Cultures were grown at 37 °C to an OD_{600} of 0.5 in L broth containing 100 μg/mL Ampicillin. Protein expression was induced by addition of 0.1 mM isopropyl-β-D-thiogalactopyranoside to the culture. Cells were harvested after 2.5 h, pelleted, resuspended in lysis buffer containing 0.1 mM Tris−HCl buffer, pH 8.5, 1 mM dithiothreitol, 5 mM benzamidine-HCl, 0.1 mM phenylmethylsulfonyl fluoride, 16 mM $MgCl_2$, and 20 mg/L DNase, and broken by three passages through a French press (SLM Instruments, Inc, Urbana, IL), with 30 s of sonication after each passage. After centrifugation at 10000*g* for 1 h, the IL-8 was found to be mainly present in the inclusion bodies. These were dissolved in 6 M guanidine−HCl, 0.1 M Tris base, and 1 mM dithiothreitol at pH 8.5 and applied to a Sephacryl S200 HR column (5 × 100cm) at a flow rate of 2 mL/min. The fractions containing monomer IL-8 were pooled. The protein was renatured by dropwise addition to 0.1 M Tris−HCl buffer, pH 8.5, containing 1 mM oxidized glutathione and 0.1 mM reduced glutathione to reach a 10-fold dilution. The renatured protein was loaded onto a HiLoad SP Sepharose 26-10 column equilibrated in 50 mM sodium acetate, pH 4.5, and was eluted with a linear gradient of 0−100% 2 M NaCl in 50 mM sodium acetate, pH 4.5. Alternatively, the renatured protein was loaded on a 15 mL S-Sepharose column and eluted in 50 mL of 2 M NaCl. The protein was dialyzed against 50 mM sodium phosphate buffer, 1.7 M ammonium sulfate, pH 7.0, loaded on a HiLoad Phenyl Sepharose column, and eluted with an ammonium sulfate gradient. Fractions containing pure IL-8 were identified by SDS−PAGE and dialyzed twice against 1% acetic acid and once against 0.1% trifluoroacetic acid prior to lyophilization. The mutant proteins were characterized by SDS−PAGE, reverse-phase HPLC, and electrospray mass spectrometry.

IL-8 Receptor Binding Assay. cDNAs encoding CXCR1 and CXCR2 were cloned (*31*) and stably transfected into Chinese hamster ovary cells as described previously (*32*). Untransfected cells were maintained in Dulbecco's modified Eagle's medium F12 containing 10% heat-inactivated fetal calf serum, and 300 μg/mL G418 was added to the media of the stably transfected cells. Membranes were prepared from the stably transfected cell lines by pelleting the cells, washing the cells in phosphate-buffered saline containing 0.02% EDTA, and resuspending the cells in 50 mM HEPES buffer containing 1 mM EDTA, 0.1 M leupeptin, 25 μg/mL Bacitracin, 1 mM phenylmethylsulfonyl fluoride, 2 μM Pepstatin A, and 10 mM $MgCl_2$, pH 7.4. The cells were broken with a Polytron homogenizer and were centrifuged at 500*g* to remove cell debris. The supernatant was centrifuged for 30 min at 48000*g* to pellet the membranes. After removal of the supernatant, the membrane pellet was resuspended in the cell lysis buffer described above and stored in aliquots at −80 °C. Scintillation proximity assays (SPA) were performed in 100 μL of 50 mM HEPES, pH 7.2, 5 mM $MgCl_2$, 1 mM $CaCl_2$, and 0.5% BSA (*33*) in 96-well plates (PET flexible 1405−401, Wallac). Membranes (1 μg/well) were incubated with 25 μg/well wheatgerm-agglutinin SPA beads, 0.1 nM [^{125}I]IL-8, and increasing amounts of nonradioactive IL-8 mutants (10^{-13}−10^{-6} M). The plates were shaken at 25 °C for at least 4 h, and the radioactivity was measured in a Wallac Microbeta Counter. Assays were performed in triplicate. The data were analyzed with GraFit Software (*34*), using the equation $B/B_{max}^{app} = 1/(1 + [L]/IC_{50})$, where B = cpm bound, B_{max}^{app} = cpm bound in the absence of competing ligand, [L] = concentration of competing ligand, and IC_{50} is the amount of unlabeled competitor required to inhibit binding by 50%. For a single-site competitive interaction, $IC_{50} = K_d + [L^*]$, where [L*] is the concentration of radiolabeled ligand added, so that under the assay conditions used, the IC_{50} approximates to the K_d (*35*).

Heparin Sepharose Chromatography. IL-8 mutants (20−50 μg) were loaded onto a 1 mL heparin Sepharose CL-6B column in 50 mM Tris−HCl, pH 7.5 buffer and eluted with a 25 mL linear gradient (0−2 M NaCl in 50 mM Tris-HCl, pH 7.5 buffer) at a flow rate of 0.5 mL/min. The protein was monitored by absorbance at 280 nm, and the concentration of NaCl was determined using an in-line conductivity meter calibrated with 50 mM Tris-HCl, pH 7.5 buffer (0% conductivity) and 2 M NaCl in 50 mM Tris-HCl, pH 7.5 buffer (100% conductivity).

Cation-Exchange Chromatography. IL-8 mutants (20−40 μg) were loaded onto a 1 mL cation-exchange column

(S−Sepharose, Fast-Flow) in 50 mM Tris-HCl, pH 7.5 buffer and eluted with a 25 mL linear gradient (0−2 M NaCl in 50 mM Tris-HCl, pH 7.5 buffer) at a flow rate of 0.5 mL/min. Protein was monitored by absorbance at 280 nm, and the concentration of NaCl was determined by using an in-line conductivity meter calibrated with 50 mM Tris-HCl, pH 7.5 buffer (0% conductivity) and 2 M NaCl in 50 mM Tris-HCl, pH 7.5 buffer (100% conductivity).

Immobilized Heparin Competitive Binding Assay. Competition experiments were performed in 96-well filter plates (Millipore MultiScreen MADVN6510, 0.65-μm pore-size, low-protein binding) in a total volume of 100 μL/well. Each well contained 0.125−0.25 nM [^{125}I]-chemokine, 5 nM unlabeled chemokine, heparin Sepharose (Sepharose beads or binding buffer as background control), and increasing amounts of heparin-derived disaccharides (0−2 mg/mL). The mass of heparin on the beads was 0.015 μg/well (corresponding to 187.5 μg of dry heparin Sepharose), and equivalent amounts of Sepharose CL-6B beads or binding buffer were used in control experiments. The plates were incubated with shaking at 25 °C for 4 h in binding buffer (50 mM HEPES, pH 7.4 containing 0.5% BSA, 5 mM $MgCl_2$, and 1 mM $CaCl_2$). The beads were washed three times with 200 μL of binding buffer containing 0.15 M NaCl under vacuum filtration. The filters were air-dried, 30 μL of scintillation fluid was added to each well, and the radioactivity was measured in a Wallac Microbeta counter. Triplicate measurements were performed for each point. The data were analyzed with GraFit Software (*34*) as described above.

NMR Spectroscopy. All NMR experiments were on Bruker AMX600 and DRX600 spectrometers using 5 mm inverse detection probes at 300 K. Titration experiments were with samples comprising 0.4 mM ^{15}N-labeled IL-8 (based on monomer subunit molecular weight) in 0.5 mL of 90% H_2O/10% D_2O containing 10 mM sodium phosphate buffer, pH 7.2. Titrations were performed by removal of the sample from the NMR tube and thorough mixing with $\leq$10 μL of a concentrated solution of disaccharide in water. Disaccharide concentrations in the titration steps were 0.1 and 0.2 mM **I**−**S**; 0.1, 0.2, and 0.4 mM **I**−**H**. Two-dimensional ^{1}H-^{15}N HSQC experiments (*36*) were acquired with spectral widths of, typically, 10 800 Hz for ^{1}H and 1824 Hz for ^{15}N; up to 256 increments were acquired in the ^{15}N dimension. A refocusing delay of 2.8 ms (corresponding to $J = 90$ Hz) was used. The solvent signal was suppressed by presaturation during the relaxation delay of 1 s. Chemical shift values were obtained via the peak picking routine within Felix (version 95.0; Molecular Simulations Inc.).

RESULTS

Purification and Activity of Mutant Proteins. Sixteen mutant IL-8 proteins, in which each of the basic residues was mutated to alanine, were produced and purified to homogeneity as determined by SDS−PAGE. These were tested for their binding to the two IL-8 receptors CXCR-1 and CXCR-2 in a scintillation proximity assay; the results are summarized in Table 1. Unlabeled wild-type IL-8 competed with the binding of [^{125}I]IL-8 to CXCR1 and CXCR2 with IC_{50} values of 1.1 and 0.2 nM, respectively. Most of the mutants were found to have IC_{50} values very similar to the wild-type IL-8 for both receptors; however, the R6A mutant had IC_{50} values that were increased about 150-fold and 2500-fold for CXCR1 and CXCR2, respectively. The R47A mutant had an approximately 10-fold higher IC_{50} for both receptors, whereas the K11A showed a 10-fold higher IC_{50} for CXCR1.

Table 1: IC_{50} Values for the Competition of [^{125}I]IL-8 from CXCR1 and CXCR2 by Unlabeled IL-8 Mutants[a]

mutant	IC_{50}, CXCR1 (10^{-9} M)	IC_{50}, CXCR2 (10^{-10} M)
wt IL-8	1.1 ± 0.7	2.1 ± 0.1
K3A	1.6 ± 0.1	7.1 ± 1.3
R6A	165 ± 15	5400 ± 1100
K11A	12 ± 0.1	7.1 ± 0.3
K15A	3.8 ± 0.6	12.5 ± 1.5
H18A	0.75 ± 0.4	4.4 ± 0.7
K20A	8.4 ± 0.9	33 ± 2
K23A	1.1 ± 0.1	3.4 ± 0.1
R26A	2.7 ± 0.1	3.7 ± 0.2
H33A	1.9 ± 0.1	2.6 ± 0.2
K42A	0.81 ± 0.3	2.3 ± 0.1
R47A	16.5 ± 1.5	28 ± 2
K54A	0.75 ± 0.24	2.1 ± 0.2
R60A	2.6 ± 0.5	6.9 ± 2.0
K64A	1.9 ± 0.5	2.2 ± 0.4
K67A	1.9 ± 0.4	2.6 ± 0.6
R68A	1.7 ± 0.5	2.1 ± 0.4

[a] The data were obtained by scintillation proximity assay performed as described in the Experimental Procedures. Each value represents the mean IC_{50} value and the SEM of at least two independent experiments performed in triplicate.

Table 2: Heparin Sepharose and Cation-Exchange Chromatography of IL-8 Mutants

IL-8 mutant	heparin Sepharose peak elution [NaCl]	Δ[NaCl]$_H$[a]	S−Sepharose peak elution [NaCl]	Δ[NaCl]$_S$[a]	$\Delta\Delta$[NaCl][b]
wt IL-8	0.59		0.47		
K3A	0.53	0.06	0.39	0.08	−0.02
R6A	0.54	0.05	0.42	0.05	0.00
K11A	0.55	0.04	0.40	0.07	−0.03
K15A	0.49	0.10	0.35	0.12	−0.02
H18A	0.57	0.02	0.44	0.03	−0.01
K20A	0.42	0.17	0.32	0.15	0.02
K23A	0.52	0.07	0.39	0.08	−0.01
R26A	0.47	0.12	0.43	0.04	0.08
H33A	0.50	0.09	0.33	0.14	−0.05
K42A	0.55	0.04	0.45	0.02	0.02
R47A	0.48	0.11	0.38	0.09	0.02
K54A	0.52	0.07	0.45	0.02	0.05
R60A	0.43	0.16	0.36	0.11	0.05
K64A	0.38	0.21	0.36	0.11	0.10
K67A	0.45	0.14	0.40	0.07	0.07
R68A	0.38	0.21	0.37	0.10	0.11

[a] Δ[NaCl] is the difference in NaCl concentration required to elute the "wild type" (wt) IL-8 compared to the mutant. [b] $\Delta\Delta$[NaCl] is the effect of the mutation on binding to heparin Sepharose after subtraction of nonspecific electrostatic effects, as determined from Δ[NaCl] on S−Sepharose; that is, $\Delta\Delta[NaCl] = \Delta[NaCl]_H - \Delta[NaCl]_S$. All concentrations are molar.

Heparin Sepharose Affinity Chromatography. The heparin-binding affinity of each of the IL-8 mutants was assessed by chromatography on heparin Sepharose; the data are summarized in Table 2. Wild-type IL-8 eluted from the heparin Sepharose column in 0.59 M NaCl under the conditions used. All of the 16 mutants showed reduced affinity compared to wild-type IL-8. For the majority of mutants elution occurred at NaCl concentrations 0.04−0.12 M lower than for the wild type. The value Δ[NaCl] was

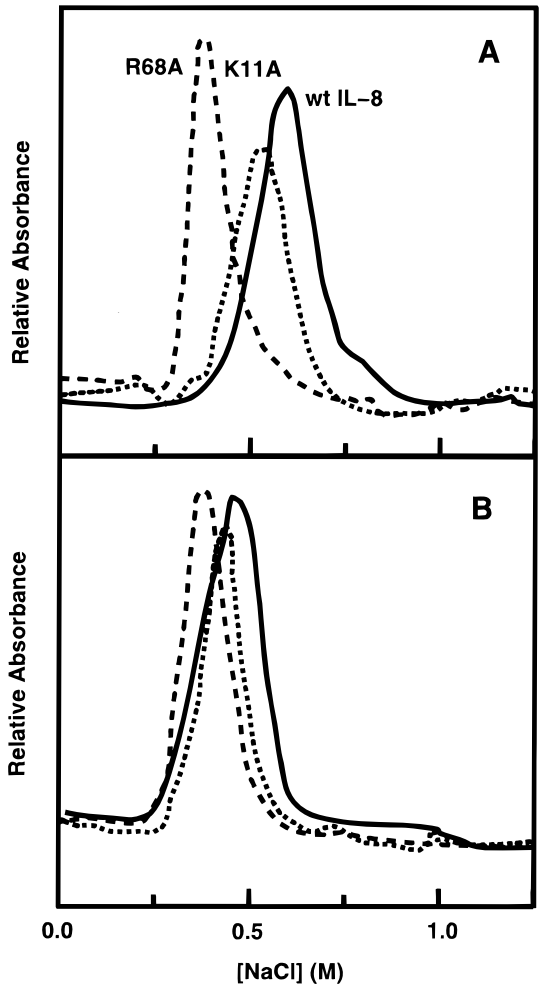

FIGURE 1: Elution profiles of the R68A (dashed line) and K11A (dotted line) mutants and wild-type IL-8 (solid line) from (A) Heparin Sepharose and (B) S−Sepharose.

calculated as the decrease in [NaCl] required for elution of the mutant protein compared to that for the wild type (Table 2). The K64A and R68A mutants showed the lowest affinity, eluting in 0.38 M NaCl, a 0.21 M reduction compared to wild-type IL-8. Mutants K20A, R60A, and K67A showed intermediate affinity for heparin Sepharose and eluted at NaCl concentrations 0.14−0.16 M lower than for wild-type IL-8. The elution profiles of the R68A mutant and of the K11A mutant, which only showed a small decrease in affinity, together with that of wild-type IL-8 are illustrated in Figure 1A.

Cation-Exchange Chromatography. The affinity of each mutant for a nonspecific cation-exchange matrix (S-Sepharose), with the same bead size as heparin Sepharose CL-6B, was estimated using the same buffer and elution conditions as for the heparin Sepharose chromatography. In these experiments the wild-type IL-8 eluted at a NaCl concentration of 0.47 M (Table 2), 0.12 M lower than required for elution from heparin Sepharose. All of the 16 single-point mutants exhibited reduced affinity for the cation-exchange column, eluting at NaCl concentrations 0.02−0.15 M less than the wild-type (Table 2). The R68A and K64A mutants, which showed considerably reduced affinity for heparin Sepharose, had a similar affinity to that of the other mutants for the cation-exchange matrix. The S-Sepharose elution profiles of the R68A and K11A mutants and of wild-type IL-8 are illustrated in Figure 1B.

Table 3: Inhibition of Binding of [^{125}I]-Labeled IL-8 to Immobilized Heparin by Disaccharides[a]

heparin-derived disaccharide [abbreviated symbol, (Sigma no.) saccharide composition]	concentration of disaccharide required to elute IL-8 (IC_{50})	*n*
I−**A**, (H 9517) (α−ΔUA-2S-[1→4]-GlcNAc-6S)	>2000 μg/mL	2
II-A, (H 8642) (α−ΔUA-[1→4]-GlcNAc-6S)	>2000 μg/mL	2
III-A, (H 8767) (α−ΔUA-2S-[1→4]-GlcNAc)	>2000 μg/mL	2
IV-A, (H 0895) (α−ΔUA-[1→4]-GlcNAc)	>2000 μg/mL	2
I−**H**, (H 8892) (α−ΔUA-2S-[1→4]-GlcN-6S)	>2000 μg/mL	2
II−**H**, (H 9017) (α−ΔUA-[1→4]-GlcN-6S)	>2000 μg/mL	2
IV−**H**, (H 9276) (α−ΔUA-[1→4]-GlcN)	>2000 μg/mL	1
I−**S**, (H 9267) α−ΔUA-2S-[1→4]-GlcNS-6S)	870 μg/mL (1.3 mM)	3
II−**S**, (H 1020) (α−ΔUA-[1→4]-GlcNS-6S)	1300 μg/mL (2.3 mM)	3
III−**S**, (H 9392) (α−ΔUA-2S-[1→4]-GlcNS)	>2000 μg/mL	2
V−**S**, (H 1145) (α−ΔUA-[1→4]-GlcNS)	>2000 μg/mL	2

[a] The immobilized heparin competition assay was performed as described in the Experimental Procedures. *n* = number of replicates. Abbreviations: ΔUA, 4-deoxy-L-threo-hex-4-enopyranosyluronic acid; GlcN = *D*-glucosamine; GalN = D-galactosamine; Ac = acetyl; NS, 2S, 6S = N-sulfate, 2-sulfate, 6-sulfate. Disaccharide nomenclature: **I**, 2S and 6S; **II**, 6S; **III**, 2S; **IV**, no 6S or 2S; **A**, GlcNAc; **H**, GlcN; **S**, GlcNS.

Specificity of IL-8 Binding by Disaccharides Derived from Heparin. A competition binding assay was used to study the interaction of IL-8 with disaccharides of defined structure that had been produced enzymatically from heparin. In this assay, heparin Sepharose beads were co-incubated with [^{125}I]-IL-8 and increasing concentrations of disaccharides. The displacement curves were fitted to a single site-binding model, and 50% inhibition concentration (IC_{50}) values were obtained. Control experiments were performed by repeating the incubations in the presence or absence of Sepharose CL-6B beads to verify the specific binding of the chemokine to the immobilized heparin (*37*). A total of eleven heparin-derived disaccharides were tested for their ability to compete with immobilized heparin in an IL-8 binding assay (Table 3); only two of these were able to compete effectively for IL-8 binding at concentrations of less than 2 mg/mL. The most effective competing disaccharides were **I**−**S**, which showed an IC_{50} of 870 μg/mL (1.3 mM), and **II**−**S**, with an IC_{50} of 1.3 mg/mL (2.3 mM).

HSQC NMR Titration Studies. The heparin-binding site on IL-8 was further investigated by titrating ^{15}N-labeled IL-8 with heparin-derived disaccharides and by monitoring chemical shift changes in ^{1}H-^{15}N HSQC spectra. Two disaccharides were chosen for the titration studies: (i) **I**−**S**, identified as having the highest affinity for IL-8 in the competition binding study, and (ii) **I**−**H**, a nonbinding disaccharide. A reference ^{1}H-^{15}N HSQC spectrum obtained from a sample of ^{15}N-labeled IL-8 at pH 7 was assigned on the basis of published values at pH 5 (*38*) together with data

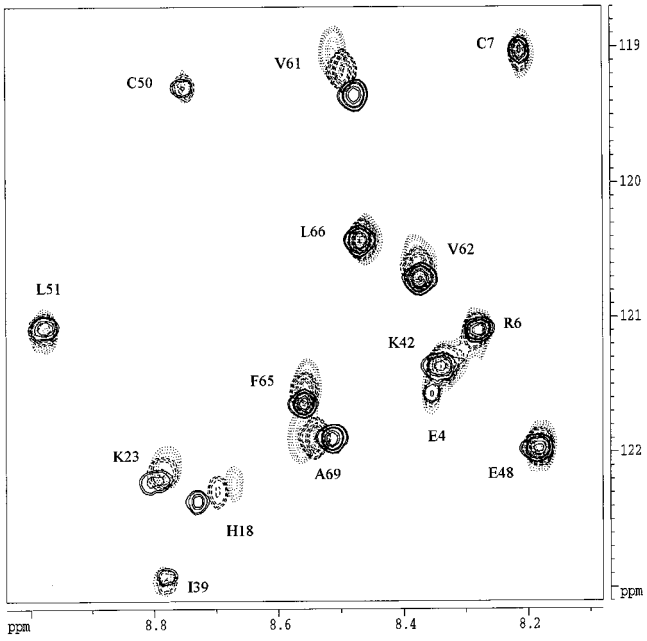

FIGURE 2: Region of ^{1}H-^{15}N HSQC NMR spectrum of ^{15}N-labeled IL-8 showing titrating and nontitrating resonances: (i) IL-8 control, no disaccharides (solid lines); (ii) IL-8 plus 0.1 mM **I**−**S** (dashed lines); and (iii) IL-8 plus 0.2 mM **I**−**S** (dotted lines).

from a pH titration study in which ^{1}H-^{15}N HSQC spectra were obtained at 0.5 pH unit intervals between pH 5 and pH 7. A total of 62 out of the 68 amide resonances from the peptide backbone of IL-8 were assigned at pH 7; the only exceptions were the resonances from the three N-terminal residues together with those from I10, S14, and N56 which were too broad to be identified under the experimental conditions.

Titration of ^{15}N-labeled IL-8 with **I**−**S** resulted in significant chemical shift changes for a number of resonances in the ^{1}H-^{15}N HSQC spectra. The differential chemical shift changes experienced by the IL-8 peptide backbone amide resonances in the presence of **I**−**S** disaccharide are illustrated clearly in Figure 2, in which an expanded region of the ^{1}H-^{15}N HSQC spectrum is shown. Thus, for example, both ^{1}H and ^{15}N chemical shifts from the V61 cross-peak titrate significantly, whereas the C50 cross-peak does not change position.

Changes of resonance positions in ^{1}H-^{15}N HSQC spectra of proteins upon ligand binding can be either upfield or downfield, and in some instances, changes are seen for either the ^{1}H or the ^{15}N chemical shift (i.e., not necessarily both) from the same backbone amide group. To "map" these effects on the protein backbone it is desirable to combine the ^{1}H and the ^{15}N data to get an overall view. In the present study, a formula used to identify significant chemical shift changes in previous HSQC titrations (*39*)

$$\Delta\delta(^{1}\mathrm{H},^{15}\mathrm{N}) = |\Delta\delta(^{1}\mathrm{H})| + 0.2|\Delta\delta(^{15}\mathrm{N})|$$

has been used to provide an appropriate weighting function to compensate for the fact that ^{15}N chemical shift changes are generally larger in magnitude than^{1}H chemical shift changes. The titration data for all of the assigned peptide backbone resonances of IL-8 in the presence of **I**−**S** (at 0.2 mM) and, separately, the nonbinding disaccharide **I**−**H** (at 0.4 mM) are presented as "weighted chemical shifts" in Figure 3. These plots demonstrate that the weighted chemical shifts for the nonbinding disaccharide **I**−**H** are all less than a value of around 0.02 ppm (the error to which chemical shifts are often quoted) and that there is no systematic variation of these values throughout the peptide backbone (Figure 3B). This disaccharide is therefore an appropriate "control" in this system as none of the IL-8 backbone resonances experience significant chemical shift changes in its presence.

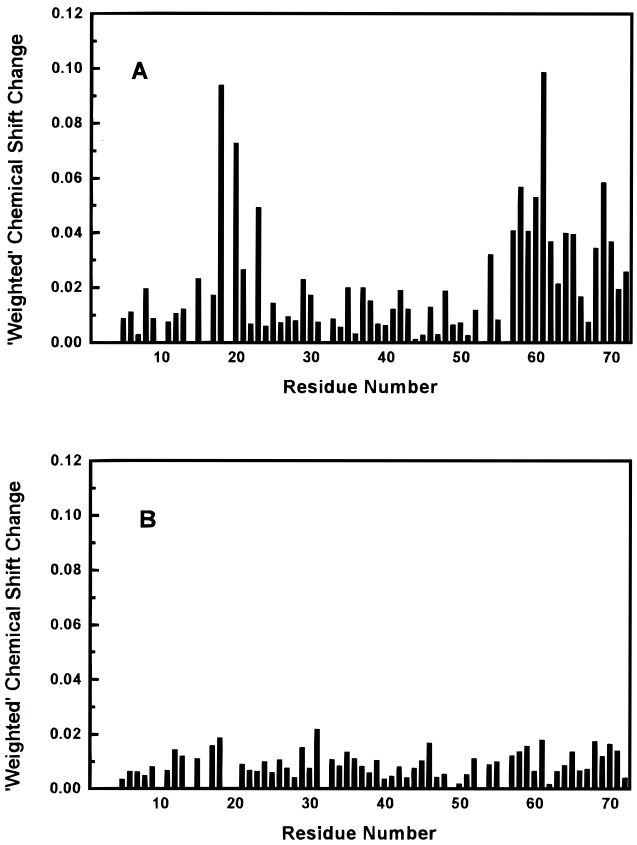

FIGURE 3: "Weighted" chemical shift changes obtained from ^{1}H-^{15}N HSQC NMR spectra for the peptide backbone signals of ^{15}N-labeled IL-8 in the presence of (A) 0.2 mM **I**−**S** and (B) 0.4 mM **I**−**H**. For details of the "weighting" applied, refer to the main text.

In contrast, the weighted chemical shifts for the IL-8-binding disaccharide **I**−**S** show a much greater range of values (Figure 3A). The largest values can be seen to be from residues that are clustered in two distinct regions of the IL-8 protein backbone: the loop region incorporating residues 18−23 and the α-helix approaching the C-terminus. Thus, significant and specific changes in the environment of the peptide backbone in these two regions of IL-8 occur upon binding of the trisulfated disaccharide.

In all of the ^{1}H-^{15}N HSQC spectra obtained in this study, a single set of signals was obtained; disaccharide binding is therefore in the "fast-exchange" regime on the chemical shift time scale, and all chemical shifts are consequently population-weighted. A further feature of the single set of signals is that the IL-8 protein is present as a dimer throughout these experiments; the cross-peaks from those residues at the dimer interface (residues 23−29) experience very small $\Delta\delta$ values even in the presence of the highest concentrations of the binding disaccharide.

DISCUSSION

The 16 basic residues of IL-8 were mutated to alanine by single-point mutagenesis to investigate the relative contribution of each to heparin binding. This contribution can be estimated from the decrease in concentration of NaCl required to elute each mutant from heparin Sepharose. The K64A and R68A mutants of IL-8 required the lowest salt concentrations for elution (Table 2, Figure 1); however, all the mutants had a reduced affinity for heparin Sepharose which was probably the result of a reduction in nonspecific electrostatic contributions to the interaction. To investigate this, the mutants were applied to S-Sepharose, a nonspecific cation-exchange matrix, under the same experimental conditions. All of the mutants eluted from the S-Sepharose at similar salt concentrations, which were lower than for wild-type IL-8 (Table 2, Figure 1); this is in contrast to the wider range of values required for elution from heparin Sepharose. The extra reduction in affinity of some of the mutants for heparin Sepharose therefore arises from an additional loss of specific electrostatic interactions. The salt concentrations required to elute each protein from the two resins can provide a measure of the level of specific over nonspecific binding when normalized with respect to wild-type IL-8. When these two values are compared for each residue (Table 2) mutations at K64 and R68 stand out as having the greatest effect on specific interactions, with smaller effects observed for mutations at K20, R60, and K67.

The specific nature of the interaction between IL-8 and heparin Sepharose was used to identify molecules that could disrupt this chemokine−GAG complex. Eleven heparin-derived disaccharides were tested, and two were found to inhibit binding with an IC_{50} lower than 2 mg/mL (Table 3). As these disaccharides successfully competed with heparin for IL-8 binding, they must retain some of the structural features required for IL-8 binding, despite their considerably reduced size and differences in their constituent monosaccharides. The disaccharides are comprised of uronate and glucosamine residues; the latter are free to mutarotate but otherwise remain unchanged from the polymeric state. The uronate residues are more extensively modified by the heparin lyase digestion, which gives rise to a partially unsaturated pyranose ring. The iduronate residues in GAGs are flexible (*40*, *41*) and this may be important for recognition; flexibility is also observed for unsaturated uronate residues of GAG disaccharides (*42*). The disaccharides used in the present study therefore retain both anionic groups and a degree of residue flexibility; consequently, they may interact with proteins in a manner similar to that of the intact GAG.

Only two heparin-derived disaccharides (**I**−**S** and **II**−**S**) were able to dissociate the IL-8−heparin complex. Disaccharide **I**−**S**, which is trisulfated, was the most effective, and these data suggest that charge density is an important requirement for interaction. Indeed, a dermatan sulfate-derived trisulfated disaccharide (which contains a di-*O*-sulfated galactosamine residue), when titrated into a solution of ^{15}N-labeled IL-8, gave rise to a very similar pattern of chemical shift changes in the ^{1}H-^{15}N HSQC spectrum to those induced by **I**−**S** (Sanderson *et al.*, unpublished data). However, the affinity was considerably reduced compared to **I**−**S** (which has the same charge density). These data suggest that the disulfated glucosamine residue of **I**−**S** is an important component of recognition. Further evidence that specificity for this interaction is not wholly driven by electrostatic charge but also arises from saccharide sequence is that, although four disulfated disaccharides were tested, only one (**II**−**S**, which also contains a disulfated glucosamine residue) was able to compete for IL-8 binding (Table 3).

The binding site of **I**−**S** on IL-8 was further characterized by NMR spectroscopy using ^{15}N-labeled protein. ^{15}N-^{1}H HSQC cross-peaks from the peptide backbone amide groups were assigned to specific residues, thereby providing a marker for almost every residue in the sequence. The addition of **I**−**S** to IL-8 produced changes in the ^{15}N and/or ^{1}H chemical shifts of resonances from several residues located within the C-terminal helix and a proximal loop (Figure 3A). The specificity of this interaction is evident from the much smaller changes for the rest of the sequence and when compared to the changes for the same cross-peaks in the presence of a nonbinding disaccharide (**I**−**H**) (Figure 3B). The perturbations in the NMR spectra are unlikely to arise from slight changes of pH during the titration as those peaks which shift the most in the presence of saccharides are not affected in control pH titrations (data not shown). Large pH-induced chemical shift changes were, however, observed for resonances from several residues (including S30 and C34) which are not significantly perturbed in the saccharide titrations.

The NMR signals that titrate to the largest extent upon binding **I**−**S** indicate residues in a "general binding region" on IL-8. A greater degree of specificity, in terms of side chain involvement in binding, cannot be obtained from the present data as the "markers" in these experiments are situated at the peptide backbone. Perturbations of these could arise through the GAG binding directly to the backbone amide in question, through the GAG binding close enough to affect the atoms electrostatically, or as a result of the secondary or tertiary structure of the protein backbone in this region being affected by binding. The small but significant changes for the NMR resonances throughout the helix (residues 57−72) may be indicative of localized changes in the structure of this region. However, the overall tertiary structure of the protein is not altered by binding of the disaccharide as evidenced by the minimal perturbations to resonances. Saccharide binding also does not appear to destabilize the dimer because the resonances of the residues at the dimer interface are not affected.

The residues of IL-8 indicated by mutagenesis and NMR to be involved in GAG binding are clustered within the C-terminal helix and the proximal loop (Figure 4). Some residues show positive effects in one experiment and not the other. For example, the mutation of K67 leads to a reduction in heparin affinity, but its NMR cross-peak does not titrate significantly. This may be due to the fact that its interaction with the GAG is via the terminal amino group and that the effects of this interaction are not transmitted to the peptide backbone. Such a phenomenon was observed for PF4 where the magnitude of perturbations to resonances from the end of side chains did not always correlate with perturbations to backbone resonances (*23*). Another anomalous residue is H18, whose resonances are perturbed in the

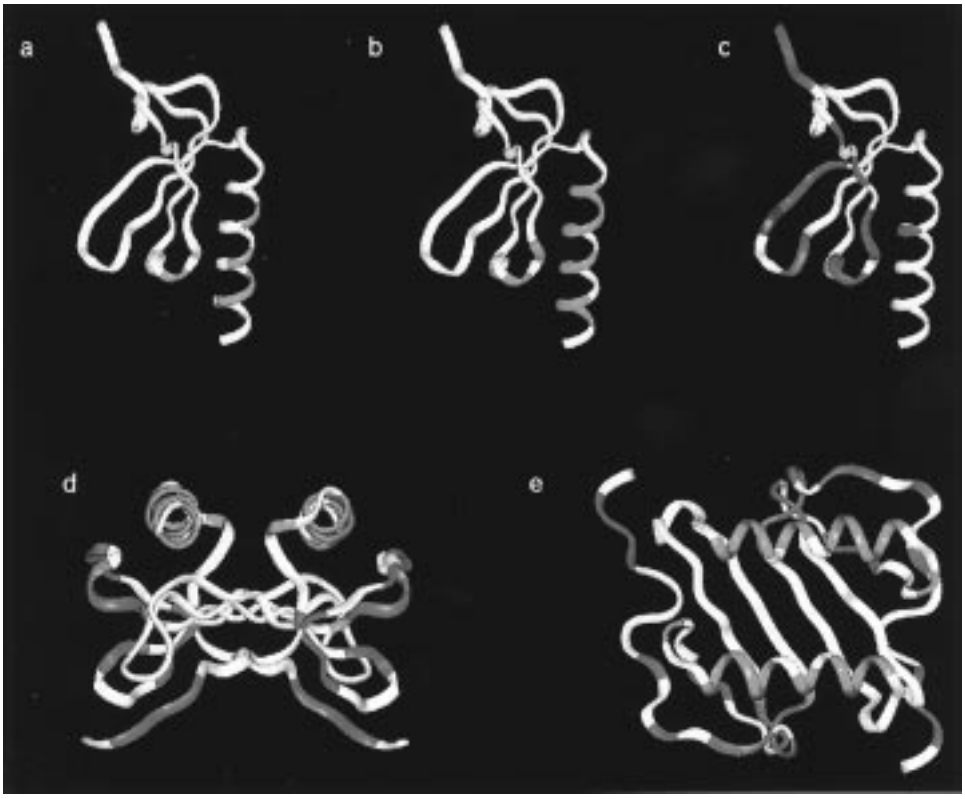

FIGURE 4: The backbone chain(s) of the IL-8 NMR structure (1il8) with the positions of the GAG- and receptor-binding residues superimposed on IL-8 monomers (a, b, c) and dimers (d, e). (a) The basic residues identified by the current mutagenesis study as contributing most to heparin binding are shown in red. (b) Residues identified by the current NMR study as showing the largest chemical shift changes induced by the IL-8-binding disaccharide **I**−**S** are shown in blue. (c) The regions of IL-8 implicated in receptor binding by mutagenesis and NMR (refs *25*, *27*, *28*, and the present study) are shown in green. The additional residue (R47) identified in the present study is indicated in brown. This residue is adjacent to the E48 to C50 sequence (*27*) and proximal to the hydrophobic epitope comprising F17, F21, I22, and L43 (*28*). (d) The spatially distinct GAG-binding surface (in red) and receptor-binding residues (in green) are highlighted; the residues of the loop that are common to both are shown in purple. (e) An orthogonal view of the dimer, with the same color scheme as in (d), indicating the relative orientations of the GAG-binding regions on the two monomers.

NMR study, but mutation of this residue shows almost no effect. The reason for this is not clear, but it is interesting that this residue has been cited as being hydrogen bonded with the loop (*21*) and may be affected by changes in the conformation of the loop.

The receptor-binding regions of IL-8 have previously been identified by mutagenesis, chemical synthesis, and NMR (*25*−*28*) and are highlighted in Figure 4c. The reduction in receptor binding observed here for the R6A mutant is consistent with previous studies (*25*, *26*, *43*). In addition it was found that mutation of R47, which had previously not been implicated in receptor binding, reduced the affinity for both IL-8 receptors 10-fold. Although mutation studies found that the triple mutant D45A, R47A, E48A had receptor binding and activity similar to those of the wild-type IL-8 (*25*), these clustered changes might not detect effects of single mutations. The R47 side chain is in close proximity to other residues involved in receptor binding (Figure 4c) and may also contribute to binding. Mutation of another neighboring residue, K20, in the present study also reduces affinity for CXCR2 by over an order of magnitude.

The GAG-binding surface of IL-8 is mostly comprised of the C-terminal helix, but residues in the proximal loop are also involved (Figure 4a,b). This loop is also implicated in receptor binding (Figure 4c); however, the GAG-interacting and receptor-binding regions can be considered to form essentially distinct surfaces on IL-8. This is particularly evident when considering the IL-8 dimer (Figure 4d). It is therefore conceivable that GAGs may have a role in presenting IL-8 to its receptor in a manner similar to that proposed for bFGF (*16*).

The NMR titrations in the present study monitored disaccharide binding to IL-8; this is in contrast to the mutant-binding experiments in which binding was to immobilized heparin polysaccharides. It may therefore seem surprising that the residues of IL-8 highlighted by the NMR experiments are more widespread than those from the mutagenesis study, but this may arise from the limitations of the NMR technique listed above or from the fact that only the basic residues were changed in the mutagenesis approach. Alternatively, the multiple interactions possible between IL-8 and the heparin polymers may restrict the orientation of the components at each site, while the disaccharide is able to sample a number of similar binding modes. The fact that the interaction with heparin does not involve residues on IL-8 that are outside the disaccharide-binding region suggests that additional contacts are not required. This is not inconsistent with models in which heparin wraps around chemokine dimers or tetramers (*20*, *24*) as, rather than forming an extensive series of contacts, the GAG may interact predominantly with the same disaccharide-binding patch on both

halves of the IL-8 dimer (Figure 4). Such interactions could promote dimerization of the chemokine in vivo. The pattern of sulfation on heparan sulfate required for IL-8 recognition may therefore be dictated by the spacing between the two disaccharide-binding regions. An analogous mechanism for the interaction between heparan sulfate and PF4 has recently been proposed (*24*).

It is interesting to note that the saccharide-binding surface on IL-8 is similar to that on PF4, in that both the C-terminal helix and the proximal loop are involved, despite differences in the positions of the basic residues. In contrast, the GAG binding region of IL-8 is quite distinct from that of another chemokine MIP-1α, which was identified by mutagenesis (*44*, *45*). This is not surprising, as although there is homology at the sequence level and in the fold of the monomers, MIP-1α is an acidic protein which has a different quaternary structure and activates different receptors on different cell types. The heparin-binding site for MIP-1α was shown to be localized to 2−4 basic residues in β-sheets, away from the α-helix, whereas the heparin-binding region on IL-8 is here shown to be at the C-terminal α-helix and the nearby H18 loop. It is worth noting, however, that the GAG-binding region of MIP-1α is a similar size to that of IL-8, and the same possibility exists for two key interaction sites per dimer, with the specificity determined by the distance between them.

In conclusion, mutagenesis and NMR experiments have highlighted a surface on IL-8 responsible for GAG binding. The region identified as involved in heparin binding is not significantly different to that for heparin-derived disaccharides, suggesting that heparin binds predominantly via highly sulfated disaccharides, with an apparent requirement for disulfated glucosamine residues. The GAG-binding region is essentially distinct from the receptor-binding region, suggesting that IL-8 could bind to its receptor in the presence of GAG. It is possible that the binding of a heparan sulfate molecule to equivalent sites on two IL-8 monomers in vivo may promote dimerization and provide a simplified model for the specificity of GAG−chemokine binding.

ACKNOWLEDGMENT

This work was supported in part by the BBSRC. We thank Christine Power and Mike Edgerton for helpful discussions and Fred Borlat for assistance with mutant purification.

REFERENCES

1. Oppenheim, J. J., Zachariae, C. O. C., Mukadia, N., and Matsushima, K. (1991) *Annu. Rev. Immunol. 9*, 617−648.
2. Larsen, C. G., Anderson, A. O., Apella, E., Oppenheim, J. J., and Matsushima, K. (1989) *Science 243*, 1464−1466.
3. Holmes, W. E., Lee, J., Kuang, W.-J., Rice, G. C., and Wood, W. I. (1991) *Science 253*, 1278−1280.
4. Tanaka, Y., Adams, D. H., Hubscher, S., Hirano, H., Sievenlist, U., and Shaw, S. (1993) *Nature 361*, 79−82.
5. Rajarthnam, K., Skyes, B. D., Kay, C. M., Dewald, B., Geiser, T., Baggiolini, M., and Clark-Lewis, I. (1994) *Science 264*, 90−92.
6. Paolini, J. F., Willard, D., Consler, T., Luther, M., and Krangel, M. S. (1994) *J. Immunol. 153*, 2704−2717.
7. Hoogewerf, A. J., Kuschert, G. S. V., Proudfoot, A. E. I., Borlat, F., Clark-Lewis, I., Power, C. A., and Wells, T. N. C. (1997) *Biochemistry 36*, 13570−13578.
8. Kjellén, L., and Lindahl, U. (1991) *Annu. Rev. Biochem. 60*, 443−475.
9. Lindahl, U., Lidholt, K., Spillmann, D., and Kjellén, L. (1994) *Thromb. Res. 75*, 1−32.
10. Gallagher, J. T., and Walker, A. (1985) *Biochem. J. 230*, 665−674.
11. Walker, A., and Gallagher, J. T. (1996) *Biochem. J. 317*, 871−877.
12. Turnbull, J. E., Fernig, D. G., Ke, Y., Wilkinson, M. C., and Gallagher, J. T. (1992) *J. Biol. Chem. 267*, 10337−10341.
13. Turnbull, J. E., and Gallagher, J. T. (1991) *Biochem. J. 273*, 553−559.
14. Lyon, M., Deakin, J. A., and Gallagher, J. T. (1994) *J. Biol. Chem. 269*, 11208−11215.
15. Ornitz, D. M., Yayon, A., Flanagan, J. G., Svahn, C. M., Levi, E., and Leder, P. (1992) *Mol. Cell. Biol. 12*, 240−247.
16. Moy, F. J., Safran, M., Seddon, A. P., Kitchen, D., Böhlen, P., Aviezer, D., Yayon, A., and Powers, R. (1997) *Biochemistry 36*, 4782−4791.
17. Faham, S., Hileman, R. E., Fromm, J. R., Linhardt, R. J., and Rees, D. C. (1996) *Science 271*, 1116−1120.
18. Ornitz, D. M., Herr, A. B., Nilsson, M., Westman, J., Svahn, C.-M., and Waksman, G. (1995) *Science 268*, 432−436.
19. Witt, D. P., and Lander, A. D. (1994) *Curr. Biology 4*, 394−400.
20. Stuckey, J. A., St. Charles, R., and Edwards, B. F. P. (1992) *Proteins: Struct. Funct., Genet. 14*, 277−287.
21. Clore, G. M., Appella, E., Yamada, M., Matsushima, K., and Gronenborn, A. M. (1990) *Biochemistry 29*, 1689−1696.
22. St. Charles, R., Walz, D. A., and Edwards, B. F. P. (1989) *J. Biol. Chem. 264*, 2092−2099.
23. Mayo, K. H., Ilyina, E., Roongta, V., Dundas, M., Joseph, J., Lai, C. K., Maione, T., and Daly, T. J. (1995) *Biochem. J. 312*, 357−365.
24. Stringer, S. E., and Gallagher, J. T. (1997) *J. Biol. Chem. 272*, 20508−20514.
25. Webb, L. M. C., Ehrengruber, M. U., Clark-Lewis, I., Baggiolini, M., and Rot, A. (1993) *Proc. Natl. Acad. Sci. U.S.A. 90*, 7158−7162.
26. Hebert, C. A., Vitangcol, R. V., and Baker, J. B. (1991) *J. Biol. Chem. 266*, 18989−18994.
27. Clark-Lewis, I., Schumacher, C., Baggiolini, M., and Moser, B. (1991) *J. Biol. Chem. 266*, 23128−23134.
28. Clubb, R. T., Omichinski, J. G., Clore, G. M., and Gronenborn, A. M. (1994) *FEBS Lett. 338*, 93−97.
29. Williams, G., Borkakoti, N., Bottomley, G. A., Cowan, I., Fallowfield, A. G., Jones, P. S., Kirtland, S. J., Price, G. J., and Price, L. (1996) *J. Biol. Chem. 271*, 9579−9586.
30. Alouani, S., Gaertner, H. F., Mermod, J.-J., Power, C. A., Bacon, K. B., Wells, T. N. C., and Proudfoot, A. E. I., (1995) *Eur. J. Biochem. 227*, 228−234.
31. Power, C. A., Meyer, A., Memeth, K., Bacon, K. B., Hoogewerf, A. J., Proudfoot, A. E. I., and Wells, T. N. C. (1995) *J. Biol. Chem. 270*, 19495−19500.
32. Lusti-Narasimhan, M., Power, C. A., Allet, B., Alouani, S., Bacon, K. B., Mermod, J- J., Proudfoot, A. E. I., and Wells, T. N. C. (1995) *J. Biol. Chem. 270*, 2716−2721.
33. Van Riper, G., Siciliano, S., Fischer, P. A., Meurer, R., Springer, M. S., and Rosen, H. (1993) *J. Exp. Med. 177*, 851−856.
34. Leatherbarrow, R. J. (1992) GraFitVersion 3.01, Erithicus Software, Staines, U.K.
35. Cheng, Y., and Prusoff, W. H. (1973) *Biochem. Pharmacol. 22*, 3099−3108.
36. Bodenhausen, G., and Ruben, D. L. (1980) *Chem. Phys. Lett. 69*, 185−188.
37. Kuschert, G. S. V., Hubbard, R. E., Power, C. A., Wells, T. N. C., and Hoogewerf, A. J. (1997) *Methods Enzymol. 287*, 369−378.
38. Grasberger, B. L., Gronenborn, A. M., and Clore, G. M. (1993) *J. Mol. Biol. 230*, 364−372.

39. Shuker, S. B., Hajduk, P. J., Meadows, R. P., and Fesik, S. W. (1996) *Science 274*, 1531−1534.
40. Sanderson, P. N., Huckerby, T. N., and Nieduszynski, I. A. (1985) *Glycoconjugate J. 2*, 109−120.
41. Ferro, D. R., Provasoli, A., Ragazzi, M., Torri, G., Casu, B., Gatti, G., Jacquinet, J.-C., Sinay, P., Petitou, M., and Choay, J. (1986) *J. Am. Chem. Soc. 108*, 6773−6778.
42. Ragazzi, M., Ferro, D. R., Provasoli, A., Pumilia, P., Cassinari, A., Torri, G., Guerrini, M., Casu, B., Nader, H. B., and Dietrich, C. P. (1993) *J. Carbohydr. Chem. 12*, 523−535.
43. Moser, B., Dewald, B., Barella, L., Schumacher, C., Baggiolini, M., and Clark−Lewis, I. (1993) *J. Biol. Chem. 268*, 7125−7128.
44. Koopman, W., and Krangel, M. S. (1997) *J. Biol. Chem. 272*, 10103−10109.
45. Graham, G. J., Wilkinson, P. C., Nibbs, R. J. B., Lowe, S., Kolset, S. O., Parker, A., Freshney, M. G., Tsang, M. L−S., Pragnell, I. B. (1996) *EMBO J. 15*, 6506−6515.

BI972867O